A Fast and Accurate Cluster Center Initialization Algorithm for PolSAR Superpixel Segmentation

Binbin Han*, Ping Han* and Zheng Cheng †
* Tianjin Key Laboratory of Advanced Signal and Image Processing, Civil Aviation University of China, Tianjin, China
E-mail: 1139199136@qq.com, hanpingcauc@163.com Tel/Fax: +86-22-24092450
† Basic Experiment Center, Civil Aviation University of China, Tianjin, China
E-mail: zcheng_10@163.com Tel/Fax: +86-15202281737

***Abstract*—Locate iterative clustering (LIC) gets good performance in superpixel segmentation for PolSAR images. However, there are also two problems in its cluster center initialization. One is that there is a lot of computational redundancy in calculating edge map, which slows down the segmentation speed. The other is that the calculated edge is much wider than the real one, which makes the fine-tuning of center seeds in 3×3 window not suitable. To solve these problems, a fast and accurate cluster center initialization algorithm for PolSAR superpixel segmentation is proposed in this paper. For the first problem, integral graph is introduced to eliminate the redundancy. For the second problem, a more reasonable window size is selected to conduct fine-tuning. Experiments with measured AIRSAR data sets demonstrate the speed of the proposed edge map calculation method increases 28 times and the center seed is farther away from the edge than before. Furthermore, LIC gets better superpixel segmentation results with the new initialization algorithm**

I. Introduction

Superpixel segmentation, as an image preprocessing step, has attracted many attentions from relevant scholars. After several years of development, many excellent approaches [1-5] has been proposed for optical images. As an outstanding representative, the simple linear iterative clustering (SLIC) shows good performance in adhering image boundaries and computational efficiency [6]. However, SLIC does not fully consider the effect of noise in its design, and can perform poorly when it's just used for polarimetric synthetic aperture radar (PolSAR) images due to the influence of strong speckle noises. Reference [7] proposed F-SLIC algorithm by replacing the spectral distance with the Euclidean distance of polarization and texture features to refine the segmentation. Reference [8] combined the decomposition-feature-iterative-clustering (DFIC) superpixel segmentation, which replaces the spectral feature with the Cloude decomposition parameter, with convolutional neural networks (CNN) to realize PolSAR images classification. Reference [9] presented a locate iterative clustering (LIC) algorithm, which improved the cluster center initialization and postprocessing step of SLIC to enhance the algorithm robustness to speckle noises, and replaced spectral distance with revised Wishart distance in the locate k-means clustering to adhere better to the image boundary. One improvement of the cluster center initialization in LIC algorithm is replacing the gradient map with the edge map, which could character the texture of images more accurately. However, there are two problems in calculating the edge map. The one is large computation, which withdraws the advantage of high computational efficiency of SLIC. The other is that the calculated edge map is much wider than the real edge, which doesn't always make the fine-tuning of cluster center in 3×3 window not on the border.

To resolve these issues, a fast and accurate cluster center initialization algorithm for PolSAR images superpixel segmentation is proposed in this paper. For the first issue, the method finds there is a lot of computational redundancy in the original calculating procedure, and this redundancy could be eliminated by integral graph. For the second issue, the method analyzes the mechanism of edge-widen effect and adopts a fine-tuning of cluster center in larger window. Experiments with measured AIRSAR data sets demonstrate the calculation time of the edge map could be reduced dramatically, the cluster center seed is farther away from the border than before. And with the new cluster center initialization algorithm, LIC get better superpixel segmentations.

II. Methodology

A. PolSAR Data

For reciprocal targets illuminated by monostatic SAR systems, the polarimetric information could be described by a complex vector

$$\mathbf{k} = \frac{1}{\sqrt{2}} \left[\begin{array}{ccc} S_{\mathrm{HH}} + S_{\mathrm{VV}} & S_{\mathrm{HH}} - S_{\mathrm{VV}} & \sqrt{2} S_{\mathrm{HV}} \end{array} \right]^{\mathrm{T}} \quad (1)$$

where S_{HV} denotes the complex scattering coefficient with horizontal transmitting and vertical receiving antenna, the others denote similarly, superscript T denotes the matrix transpose. Generally, PolSAR data is not directly represented with this complex vector, but with the outer product of the associated target vector with its conjugate transpose

$$\mathbf{T} = \langle \mathbf{k} \bullet \mathbf{k}^{\mathrm{H}} \rangle = \frac{1}{L} \sum_{i=1}^{L} \mathbf{k}_i \mathbf{k}_i^{\mathrm{H}} \quad (2)$$

where $\langle \cdots \rangle$ indicates temporal or spatial ensemble averaging, assuming homogeneity of the random medium, and this conduction is the well-known multi-look process, superscript H indicates conjugate transpose. L is the number of multi-look.

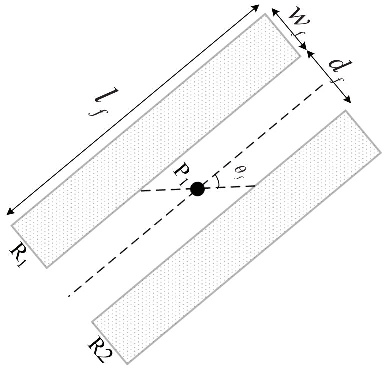

Fig. 1. The edge detector model characterized by the configuration $K_f = \{l_f, w_f, d_f, \theta_f\}$.

B. LIC Algorithm

LIC is an improved method of SLIC for the application of PolSAR images superpixel segmentation. The basic procedure of this algorithm mainly consists of three steps: 1) filter preprocessing and cluster centers initialization; 2) local iterative clustering; 3) postprocessing.

In the first step, multi-look and/or speckle filtering is applied to the original PolSAR data to suppress the speckle noise. And then the edge map is calculated by a set of edge detector models [10] with different orientations showing as Fig. 1. For each pixel, calculate the hypothesis test distance between regions R_1 and R_2 with different orientations θ, find and save the maximum distance $D_{\max}$ and its corresponding θ as this pixels edge value. The edge-map is obtained by repeating this procedure for every pixels in PolSAR image. The hypothesis test distance is defined as [11]

$$d_{\mathrm{HT}}\left(R_i, R_j\right) = \left(N_i + N_j\right) \ln \left|\widehat{\boldsymbol{\Sigma}}\right| - N_i \ln \left|\widehat{\boldsymbol{\Sigma}}_i\right| - N_j \ln \left|\widehat{\boldsymbol{\Sigma}}_j\right| \quad (3)$$

Where N_i and N_j are the number of samples in regions R_i and R_j. $\widehat{\boldsymbol{\Sigma}}_i$ and $\widehat{\boldsymbol{\Sigma}}_j$ are the center coherence matrix of R_i and R_j region, $\widehat{\boldsymbol{\Sigma}}$ is the center coherence matrix of these two regions, they can be calculated as

$$\widehat{\boldsymbol{\Sigma}}_i = \frac{\sum_{n=1}^{N_i} \mathbf{T}_n}{N_i}, \widehat{\boldsymbol{\Sigma}}_j = \frac{\sum_{n=1}^{N_j} \mathbf{T}_n}{N_j}, \widehat{\boldsymbol{\Sigma}} = \frac{N_i \widehat{\boldsymbol{\Sigma}}_i + N_j \widehat{\boldsymbol{\Sigma}}_j}{N_i + N_j} \quad (4)$$

With the edge map, the center seed moves to the lowest edge position in 3×3 local window to avoid the effect of textures and noises. Furtherly, LIC proposes a grid-centered clustering strategy to initialize the cluster label and minimum distance of each pixel.

In the second step, LIC replaced the spectral distance with the revised Wishart distance. With the combining distance of revised Wishart and spatial, the algorithm accomplished the local iterative clustering. These distances can be represented

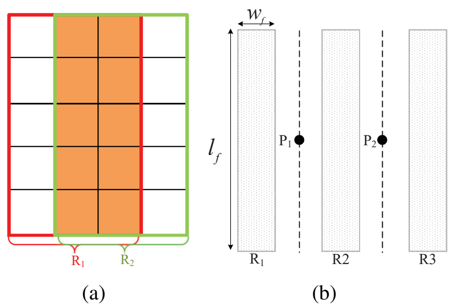

Fig. 2. The sketch map of redundancy analysis. (a) redundancies in regions, (b) redundancies in edge detector models.

as

$$\begin{cases} d_{\mathrm{RW}} = \ln\left(\frac{|\widehat{\boldsymbol{\Sigma}}_j|}{|\mathbf{T}_i|}\right) + \operatorname{Tr}\left(\widehat{\boldsymbol{\Sigma}}_j^{-1}\mathbf{T}_i\right) - q \\ d_s = \sqrt{\left(x_i - x_j\right)^2 + \left(y_i - y_j\right)^2} \\ D = \sqrt{\left(\frac{d_{\mathrm{RW}}}{m}\right)^2 + \left(\frac{d_s}{S}\right)^2} \end{cases} \quad (5)$$

Where d_{RW} is the revised Wishart distance, and d_s is the spatial distance. $\operatorname{Tr}(\cdots)$ denotes the matrix trace operation. q is a constant and its value is 3 in this paper, (x_i, y_i) and (x_j, y_j) are the coordinates of current pixel and clustering center, respectively. m is a parameter controlling the relative weight between d_{RW} and d_s. S is the expected size of a superpixel.

In the third step, the superpixel, whose region size is in $[N_{\min}, N_{\max})$ and dissimilarity with its neighborhood superpixel is smaller than G_{th}, will be merged into its adjacent superpixel. The dissimilarity measure is defined as

$$G = \frac{1}{q}\left\|\frac{\mathbf{T}_i^{\mathrm{diag}} - \mathbf{T}_j^{\mathrm{diag}}}{\mathbf{T}_i^{\mathrm{diag}} + \mathbf{T}_j^{\mathrm{diag}}}\right\|_1 \quad (6)$$

Where $\mathbf{T}_i^{\mathrm{diag}}$ denotes the vector composed by the diagonal elements of superpixel central coherence matrix. $\|\cdots\|_1$ denotes the 1-norm.

C. Proposed Cluster Center Initialization

1) Fast Edge Map: One problem of LIC initialization is that there is a lot of redundancy in calculating the edge map. As shown in Fig. 2(a), One redundancy lies in the center calculating of regions, when the region centers of red and green window are computed successively, pixels marked with brown background are the redundancies. Another redundancy lies in the edge detector model. As shown in Fig. 2(b), the region center of R_2 region is computed twice when calculating the edge value of P_1 and P_2 pixel, respectively.

To reduce the computation redundancy, integral graph is introduced in this paper. The advantage of this process reflects in three aspects: 1) The computational complexity within a single region is obviously reduced. 2) The redundancy of the edge detector model is avoided by calculating the integral map on a whole expanded image. As shown in Fig. 3, regions over and under the center pixel correspond to the integral graph marked as red and green, respectively. Most areas of these

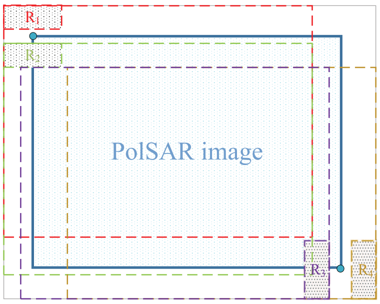

Fig. 3. The sketch map of calculating edge map fast.

two integral maps are overlap, and they can be calculated once on the expanded image. 3) The redundancy within edge detector models, whose orientation difference is 90°, can also be avoided. Regions on the left and right of the center pixel correspond to the integral graph marked as purple and brown in Fig. 3, these regions are similar to the above two, and they can be transformed to each other by interchanging the length and width.

In many applications, setting the number of orientations to 4, namely $\{0°, 45°, 90°, 135°\}$, is enough. In this case, only the integral graph with 0° and 45° directions need to be calculated. The integral graph with 0° direction can be calculated as [12]

$$\begin{aligned} S_{\mathrm{IR}}(i,j) = S_{\mathrm{IR}}(i,j-1) + S_{\mathrm{IR}}(i-1,j) \\ +I(i,j) - S_{\mathrm{IR}}(i-1,j-1) \end{aligned} \tag{7}$$

where $S_{\mathrm{IR}}(i,j) = \sum_{i' \le j, j' \le j} I(i',j')$ is the sum of the pixels of the rectangle ranging from the top left corner at $(0,0)$ to the bottom right corner at (i,j), and $S_{\mathrm{IR}}(-1,j) = S_{\mathrm{IR}}(i,-1) = 0$. For PolSAR images, $I(i,j)$ is the coherency matrix $\mathbf{T}$ with coordinate (i,j). From this integral graph, the pixel sum of the region can be determined as

$$\begin{aligned} S_{\mathrm{R}}(i,j,l,w) = S_{\mathrm{IR}}(i-1,j-1) + S_{\mathrm{IR}}(i+l-1,j+w-1) \\ -S_{\mathrm{IR}}(i-1,j+w-1) - S_{\mathrm{IR}}(i+l-1,j-1) \end{aligned} \tag{8}$$

where l and w are the length and width of the region, respectively. For the integral graph with 45° direction, it can be calculated with two passes over all pixels. The first pass from left to right and top to bottom determines

$$\begin{aligned} S_{\mathrm{RIR}}(i,j) = S_{\mathrm{RIR}}(i-1,j-1) + S_{\mathrm{RIR}}(i-1,j) \\ +I(i,j) - S_{\mathrm{RIR}}(i-2,j-1) \end{aligned} \tag{9}$$

where $S_{\mathrm{RIR}}(i,j) = \sum_{i' \le i, |j'-j| \le i-i'} I(i',j')$ and $S_{\mathrm{RIR}}(-1,j) = S_{\mathrm{RIR}}(-2,j) = S_{\mathrm{RIR}}(i,-1) = 0$. The second pass from the right to left and bottom to top calculates

$$S_{\mathrm{RIR}}(i,j) = S_{\mathrm{RIR}}(i,j) + S_{\mathrm{RIR}}(i-1,j+1) - S_{\mathrm{RIR}}(i-2,j) \tag{10}$$

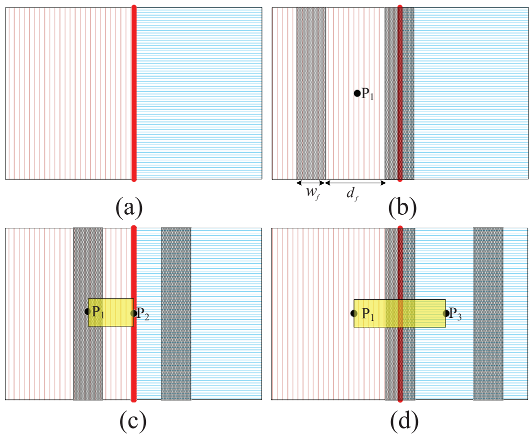

Fig. 4. The sketch map of edge-broaden effect. (a) Two regions marked with red vertical and blue horizontal stripes, (b) Edge detector model at P_1, (c) Edge detector model at P_2, (d) Edge detector model at P_3.

From this integral graph, the pixel sum of the region can be determined as

$$\begin{aligned} S_{\mathrm{RR}}(i,j,l,w) = S_{\mathrm{RIR}}(i+l,j+l) + S_{\mathrm{RIR}}(i-w,j+w) \\ -S_{\mathrm{RIR}}(i,j) - S_{\mathrm{RIR}}(i+l-w,j+l+w) \end{aligned} \tag{11}$$

2) Fine-tuning of the Center Seed: The edge-widen effect can be illustrated as Figure 4. Shown as Figure 4(a), there are two regions marked with red vertical stripes and blue horizontal stripes, respectively, the red line is the real edge of these two regions. As the edge detector model moving from pixel P_1 through P_2 to P_3 , and the calculated edge is obtained, which is shown as a yellow rectangle and its width is $d_f + w_f$. Compared with the real edge, the calculated edge is obviously wider.

In order to ensure the center seed not lies on the border or noise pixel, the fine-tuning of cluster center needs to be conducted in a larger window, which is set to $(d_f + w_f + 1) \times (d_f + w_f + 1)$.

The center seed may moves to the outside of the regular grid when the original center is sampled on the regular grid border, it is reasonable to add an inspection process in the initialization. In this paper, the inspection process is designed as: setting the maximum sampling times T, the center seed is the pixel determined by $(d_f + w_f + 1) \times (d_f + w_f + 1)$ window if it's not located on the outside of the regular grid within T times, else the center seed is the lowest edge-value pixel in the regular grid.

3) Initialization of Cluster Center Seeds: On the basis of above, the initialization of cluster center can be summarized as following,

Step 1: set the sampling times T and fine-tuning window $(d_f + w_f + 1) \times (d_f + w_f + 1)$.

Step 2: calculate the edge map with the fast method.

Step 3: get the original cluster center seed by sampling on a regular grid, with the interval S, and then move it to the lowest edge position in $(d_f + w_f + 1) \times (d_f + w_f + 1)$.

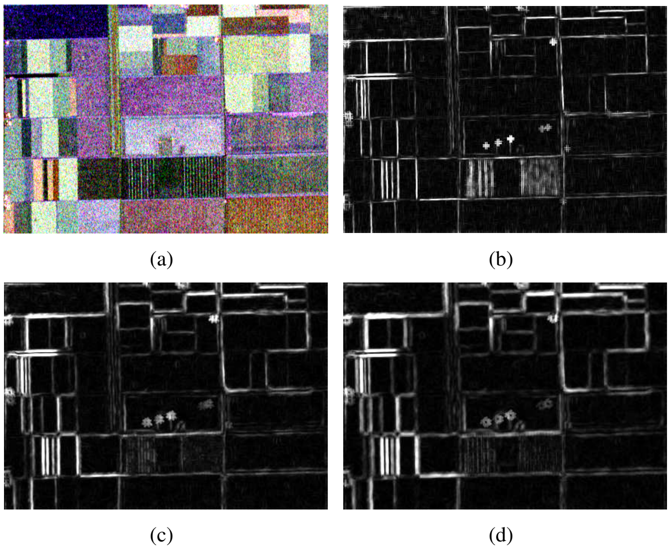

Fig. 5. The PauliRGB image and edge map with different parameter $\{l, w, d\}$. (a) Original PauliRGB image,(b) Edge map with $\{9, 1, 1\}$, (c) Edge map with $\{9, 3, 1\}$, (d) Edge map with $\{9, 3, 3\}$.

Step 4: check whether the center seed is in the regular grid, if not and the sampling times is less than T turn to step 3, if sampling times is equal or more than T, turn to step 5, else turn to step 6.

Step 5: set the center of the regular grid as the original cluster center seed, and move it to the lowest position in $S \times S$.

Step 6: save the result of step 4 and 5 as the current center seed, and repeat above steps on the other regular grid.

III. Experiments

In this section, the performance of the proposed cluster center initialization algorithm for PolSAR superpixel segmentation is presented and analyzed on the real data set obtained by AIRSAR airborne platform on August 16, 1989. The experimental image is shown in Figure 5(a), the size of which is 425×299 and the resolution is 6.7m in range direction, 12.1m in azimuth direction. The scene covers Flevoland, Netherlands. The main contents of this area are farmlands, and the edge of which is clear and regular. These characters make it suitable for edge analyzing.

A. Edge Map Results and Analysis

The experiments are conducted with a single CPU (3.0GHz i5) on Matlab (2015a). The edge map under different detector model parameters is shown in Fig. 5, and the operation time is listed in Tab. 1. For clearly displaying the edge, the brighten function of Matlab is used on these edge maps. As shown in Fig. 5, the calculated edge becomes wider as the width and distance of regions increase, this result is consistent with the analysis above. With different parameters, all of the operation time of original LIC algorithm are nearly 200 seconds, whereas they are nearly 7 seconds with the proposed method, the computational complexity is reduced by about 28 times.

TABLE I
Comparison of the Operation Time with Different Detector Parameters

Algorithms and increased ratio	Under different conditions of detector $\{l, w, d\}$		
	$\{9, 1, 1\}$	$\{9, 3, 1\}$	$\{9, 3, 3\}$
LIC	192.7s	196.9s	197.5s
The proposed	6.9s	6.9s	7.1s
Increased ratio	27.9	28.5	27.7
Average ratio	28.0		

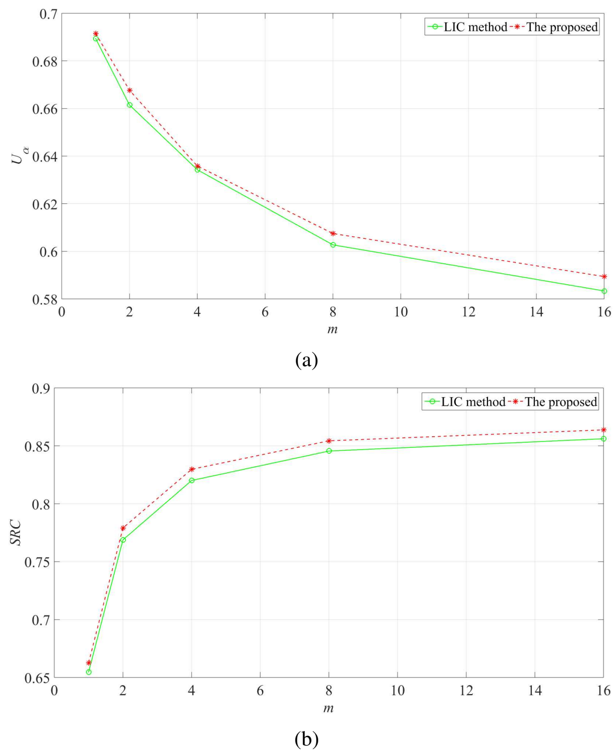

Fig. 6. Comparison of LIC and proposed method with different weight m. (a) Comparison of Homo, (b) Comparison of SRC

B. Superpixel Segmentation Results and Analysis

In order to conveniently compare the superpixel segmentation performance of different methods, the evaluation index U_α proposed by [13] and SRC proposed by [14] are used to quantitatively evaluate the homogeneity and shape regularity of superpixels, their values range from 0 to 1, and the larger their value, the better the superpixel segmentation. The segmentation results of Reference [6] (marked as SLIC), Reference [7] (marked as F-SLIC), Reference [8] (marked as DFIC) and Reference [9] (marked LIC) are also presented. The weight parameter m of SLIC is set as 40, and the other methods are set as the same one with their papers. The proposed method here means the superpixel segmentation algorithm with the proposed initialization, LIC iterative clustering and postprocessing strategy. The weight factor m is set as 1.

Since this method is an improved initialization algorithm for LIC, and different feature combinations should corre-

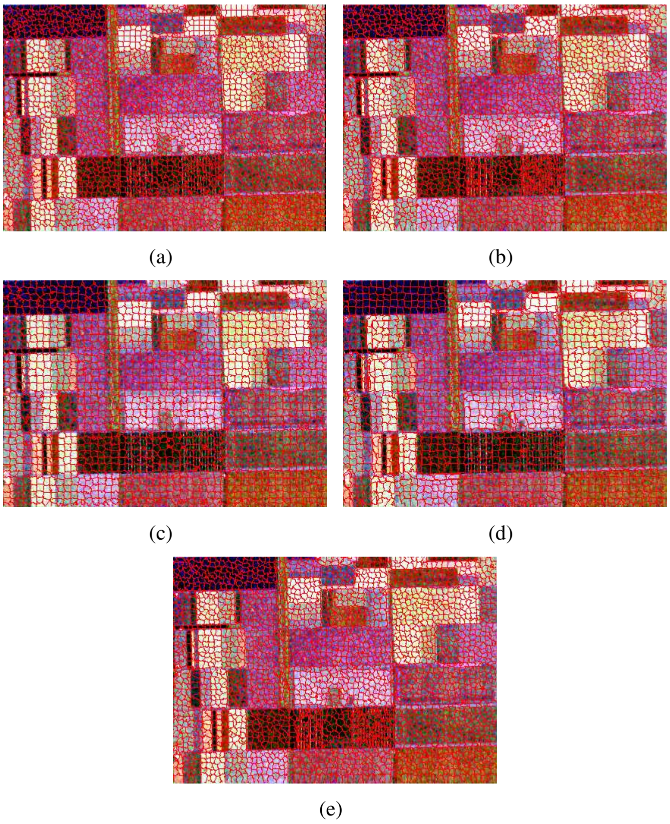

Fig. 7. Comparison of the superpixel segmentation results. (a) SLIC, (b) LIC, (c) DFIC, (D) F-SLIC, (e) The proposed.

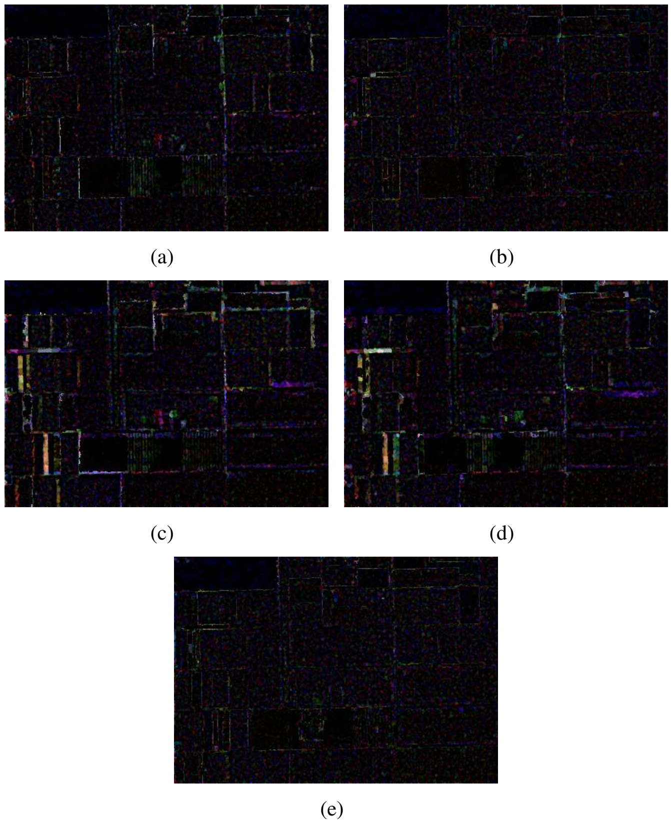

Fig. 8. Differential map of the original and superpixel segmentation image. (a) SLIC, (b) LIC, (c) DFIC, (D) F-SLIC, (e) The proposed.

sponds to different the weight factors. The robustness of LIC and proposed method under different weight factors, as $m = \{1, 2, 4, 8, 16\}$, is analyzed, and other methods are not presented. Fig. 6 shows the results. Because there is a random sampling process in the initialization, the experiment under each m is repeated 20 times. U_α becomes smaller as m increases, whereas SRC becomes larger. The choose of m is a balance procedure of the contradiction between U_α and SRC. U_α and SRC of the proposed method are higher than that of LIC algorithm at each m, which indicates the proposed method improved the superpixel segmentation results.

The detailed superpixel segmentation results of SLIC, LIC, DFIC, F-SLIC and the proposed method are presented in Fig. 7 and Fig. 8. Images in Fig. 7 show the boundaries of superpixels, which are marked with red lines. Compared with Fig. 7(a), (b) and (e), the shape of the superpixels of Fig. 7(c) and (d) is more regular and the area of the superpixels is more intensive, because these two methods adopted a relatively larger m value and no sampling procedure within the regular grid in their papers. Fig. 8 shows the differential map of the original and superpixel segmentation image. The closer the map is to black images, the smaller the difference between the original and segmentation. Comparing these five maps, the smoothing effect of DFIC and F-SLIC are most serious, SLIC and LIC rank second, and the proposed method preserved the original image best.

TABLE II
THE RUNNING TIME OF DIFFERENT ALGORITHMS

Algorithms	Running time
DFIC	175.7s
LIC	264.3s
F-SLIC	180.0s
The proposed	68.7s

The running time of DFIC, F-SLIC, LIC and the proposed algorithm is listed in Tab. 2. Since SLIC algorithm is encoded with C++, its running time is not listed here. As seen from Tab. 2, the running time of LIC changes from the most to the least with the proposed initialization algorithm, which demonstrates the effectiveness of the proposed method.

IV. Conclusion

LIC algorithm introduced SLIC algorithm into PolSAR images superpixel segmentation and improved the segmentation results. However, there are also two problems, one is computational redundancy in calculating edge maps, the other is edge-widen effect. The main contribution of this paper is improving the cluster center initialization method. The effectiveness of the improved algorithm is demonstrated by AIRSAR data sets.

V. Acknowledgment

This work was supported by the National Natural Science Foundation of China (No.61571442) and the National Key Research and Development Program of China (No. 2016YFB0502405). And the authors would like to thank the PolSARpro project for providing the open-source software and experimental data (as distributed by the European Space Agency).

References

[1] X. Ren and J. Malik, " Learning a classification model for segmentation," *9th IEEE International Conference on Computer Vision. Washington, DC, USA*, vol.2, pp. 10-17, 2003.

[2] J. Shi and J. Malik, " Normalized cuts and image segmentation," *IEEE Trans. Pattern Analysis and Machine Intelligence*, vol. 22, no. 8, pp. 888-905, Aug. 2000.

[3] P. Felzenszwalb and D. Huttenlocher, "Efficient graph-based image segmentation," *International Journal of Computer Vision*, vol. 59, no. 2, pp. 167-181, Sep. 2004.

[4] A. Levinshtein, A. Stere, K. Kutulakos, D. Fleet, S. Dickinson and K. Siddiqi, "TurboPixels: fast superpixels using geometric flows," *IEEE Transactions on Pattern Analysis and Machine Intelligence*, vol. 31, no. 12, pp. 2290-2297, Dec. 2009.

[5] V. Michael, B. Xavier, R. Gemma and V. Luc, "SEEDS: superpixels extracted via energy-driven sampling," *International Journal of Computer Vision*, vol. 111, no. 3, pp. 298–314, Feb. 2015.

[6] R. Achanta, A. Shaji, K. Smith, A. Lucchi, P. Fua and S. Ssstrunk, "SLIC superpixels compared to state-of-the-art superpixel methods," *IEEE Transactions on Pattern Analysis and Machine Intelligence*, vol. 34, no. 11, pp. 2274-2282, Nov. 2012.

[7] L. Zhang, C. Han and Y. Cheng, "Improved SLIC superpixel generation algorithm and its application in polarimetric SAR images classification," *2017 IEEE International Geoscience and Remote Sensing Symposium, Fort Worth, TX, USA*, pp. 4578-4581, Jul. 2017.

[8] B. Hou, C. Yang, B. Ren and L. Jiao, "Decomposition-Feature-Iterative-Clustering-Based Superpixel Segmentation for PolSAR Image Classification". *IEEE Geoscience and Remote Sensing Letters*, vol. 15, no. 8, pp. 1239-1243, Aug. 2018.

[9] F. Qin, J. Guo and F. Lang, "Superpixel segmentation for polarimetric SAR imagery using local iterative clustering," *IEEE Geoscience and Remote Sensing Letters*, vol. 12, no. 1, pp. 13-17, Jan. 2015.

[10] J. Schou, H. Skriver, A. Nielsen, and K. Conradsen, "CFAR edge detector for polarimetric SAR images," *IEEE Transaction Geoscience Remote Sensensing*, vol. 41, no. 1, pp. 20C32, Jan. 2003.

[11] P. Formont, F. Pascal, G. Vasile, J. Ovarlez and L. Ferro-Famil, "Statistical Classification for Heterogeneous Polarimetric SAR Images," *IEEE Journal of Selected Topics in Signal Processing* , vol. 5, no. 3, pp. 567-576, Jun. 2011.

[12] R. Lienhart and J. Maydt, "An extended set of Haar-like features for rapid object detection," *International Conference on Image Processing. Rochester, NY, USA*, vol. 1, pp. I-900. Feb. 2002.

[13] C. Han, "Superpixel segmentation method for high resolution PolSAR images (Master Thesis)," *Harbin Institute of Technology*, Harbin, China, 2017.

[14] R. Giraud, V. Ta and N. Papadakis, "Robust shape regularity criteria for superpixel evaluation,"*2017 IEEE International Conference on Image Processing, Beijing, China*, , pp. 3455-3459, Sep. 2017.